NUMERICAL SIMULATION OF BUILDING-INTEGRATED PHOTOVOLTAIC SYSTEMS

Roberto Z. Freire†, roberto.freire@pucpr.br
Industrial and Systems Engineering Graduate Program - PPGEPS

Marc O. Abadie, mabadie@univ-lr.fr
LEPTIAB - University of La Rochelle - 17000 La Rochelle - France

Nathan Mendes†, nathan.mendes@pucpr.br
Mechanical Engineering Graduate Program - PPGEM/LST

† - Pontifical Catholic University of Parana - PUCPR
Rua Imaculada Conceição, 1155. Curitiba/PR/Brazil - Zip Code 80215-901

Abstract. *Many technologies to convert solar energy into electricity have been proposed in literature, but the advances in the photovoltaic conversion are evident. The costs reduction, increasing efficiency, reducing the needed area and generic applicabilities have been used as attractive issues for photovoltaic systems. Based on these concepts, this work treats the simulation of BIPV (building-integrated photovoltaic systems) and describes a simplified model capable to calculate the thermal interactions between the building structure and photovoltaic crystalline modules. This photovoltaic model was implemented into a whole-building and energy simulation software, providing an additional functionality in terms of building simulation. Moreover, an incidence angle modifier algorithm was also implemented, and verification procedures, showing the solar to electrical energy conversion in comparison to the TRNSYS software, were used to validate the implementation of the photovoltaic model.*

Keywords: *Solar Energy, Photovoltaic Systems, BIPV, Building Simulation.*

1. INTRODUCTION

In recent years, the whole world has been experiencing a growing electricity demand and a decrease of available resources to expand the generation system. Due to many facts as population and economic growth and access to cheaper electrical appliances, that have only recently become available, interests in the potential of renewable energy and passive technology integration have been taken place between academic and industrial researches.

Among different ways to generate electricity, the use of solar energy for the industrial, public, commercial and residential sectors has been discussed in many countries as one of the possible solutions to reduce global warming, since energy generated by fossil fuel combustion can be avoided. Electricity produced using the Sun's energy reduces the amount of energy used from non-renewable resources such as coal, gas, oil and nuclear. Additionally, when small solar energy conversion systems are considered in buildings applications, energy is not wasted, *e.g.* as in transmission losses. Moreover, there are significant environmental benefits resulting from reductions in air pollution from burning fossil fuels, reductions in water and land use from central generation plants, reductions in the storage of waste byproducts. In addition, the solar technologies produce energy with little noise and few moving parts.

As presented before, small photovoltaic systems can be associated to buildings and contribute to reduce the net energy demand. In the Brazilian context, some studies in order to motivate the use of PV systems are being developed. Considering the amount of solar energy which reaches the Brazilian surface (see Fig. 1), an insignificant parcel is converted to electrical energy - less than 0.1% (EPE, 2009).

One example which motivates the use of photovoltaic systems in the Brazilian context has been presented by Silva and Beyer (2008), which associates the PV technology to a HVAC system providing a cost analysis and a design methodology of PV systems using the EnergyPlus simulation software. According to Silva and Bayer results, considering the whole HVAC system as energy demand for the PV system and high thermal loads for the indoor environment are not economically viable and low costs and small PV systems are considered the correct choice for the Brazilian economy.

Considering that almost 45% of the total energy demand in Brazil can be attributed to Buildings (EPE, 2009), this work presents the integration of a photovoltaic module into a whole building and energy simulation software - PowerDomus (Mendes *et al.*, 2003), which is capable to associate the building energy demand systems to the photovoltaic module and reduce the energy required from the net.

It can be verified that most residential photovoltaic systems are used in conjunction with utility-supplied power and, in addition to the PV panels, an inverter, located near the electrical panel, converts the PV produced electricity into utility compatible alternating current (AC) electricity for the building. When storage systems are used, it can be possible to provide electricity for the building even when the utility power is disconnected or when the sun is not shining. The main

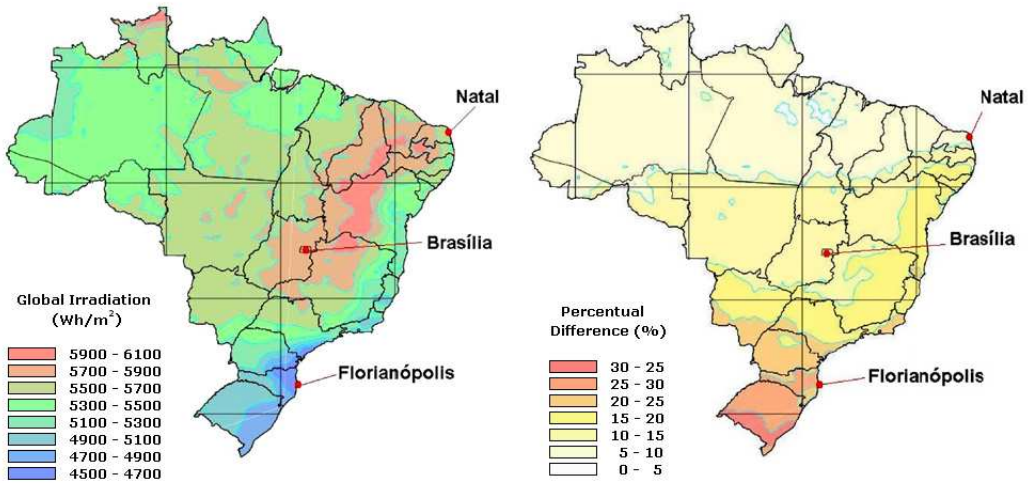

Figure 1. Brazilian solar atlas - yearly average of the daily global radiation and its percentage variation on horizontal plane (Ordenes *et al.*, 2007).

objective of this work is to describe a simplified way to integrate both PV array and building structure and verify the hygrothermal interactions between them. In this way, inverters and storage systems are not described here and will be discussed in future works.

Many types of models are available to evaluate a considerable range of parameters related to PV systems. Some of the most disseminated models are presented in (Friling *et al.*, 2009; CETC, 2004; Davis *et al.*, 2002; PHANTASM, 1999). As it can be verified on the previous cited works, many objectives can be found on the PV research area, since models capable to verify the influences of the outdoor climate conditions on the physical parameters of PV systems, *e.g.*, changes on cell efficiency due to temperature variations, until models capable to describe the payback time of PV systems when integrated to buildings. Among many PV simulation software, one should cite RETSCreen (CETC, 2004) and PVSYST (ISE, 2008), which are considered software packages - worldwide used - for the technical study, sizing, simulation and data analysis of photovoltaic systems.

However, when a more detailed analysis is required, and the integration of both building structure and photovoltaic panels must be verified, the software has to provide the whole-building and energy simulation reports. This is a reduced group of software such as EnergyPlus (Griffith and Ellis, 2004), TRNSYS (Solar Energy Laboratory, 2007) and ESP-r (Qiu *et al.*, 2009). In this way, the present work proposes an implementation of a photovoltaic module into a building hygrothermal and energy simulation software.

This work is dived as follows: the next sections presents the mathematical model which describes the photovoltaic solar to electrical energy conversion. In Section 3, the building model is presented. The photovoltaic module integration to the building structure is presented in Section 4 and, in Section 5, the verification procedures are presented and then the conclusions are addressed.

2. ARRAY MODELING

The photovoltaic model for crystalline PV modules (either single crystal or polycrystalline technology), which has been incorporated into PowerDomus, was developed largely by Townsend (1989) and also detailed by Duffie and Beckman (1991). The four-parameter equivalent circuit model is also available in TRNSYS PV component (Eckstein, 1990). It is called "four-parameter" because it estimates from available data the values of four parameters that cannot be obtained directly from manufacturers' catalogs.

To enhance the algorithm precision, it also includes an optional incidence angle modifier correlation to calculate how the reflectance of the PV module surface varies with the angle of incidence of solar radiation. Based on well established PV simulation codes, the algorithm also determines the PV current as a function of load voltage. The four-parameter equivalent circuit is shown in Fig. 2.

During the whole-building and energy simulation, the array efficiency must be calculated at each time step. This value can be obtained dividing the amount of energy that reach the panel surface by the total energy converted into electrical power as shown in Equation 1:

$$\eta_c = \frac{E_p}{(G_T \; y_1 \; y_2)}, \tag{1}$$

where η_c is the collector efficiency, E_p the power at the array output (W), G_T is the total irradiance that reaches de panel

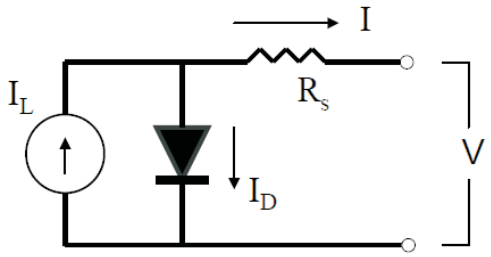

Figure 2. Equivalent electrical circuit in the four-parameter model.

surface (W/m^2) and y_1 and y_2 the array width and length (m).

2.1 Determining Performance under Operating Conditions

The current-voltage characteristics of a PV change with both insolation and temperature. The PV model employs these environmental conditions along with the four module constants $I_{L,ref}$, $I_{o,ref}$, γ, and R_s to generate an IV curve at each time step. The current-voltage equation of circuit shown in Fig. 2 is as follows:

$$I = I_L - I_o \left[\exp\left(\frac{q}{\gamma \, \lambda_c \, T_c} (V + I + R_s) \right) - 1 \right], \tag{2}$$

where R_s γ and λ_c are constants. The photocurrent I_L depends linearly on incident radiation:

$$I_L = I_{L,ref} \frac{G_T}{G_{T,ref}} \tag{3}$$

The reference insolation $G_{T,ref}$ is a model input parameter. It is nearly always defined as $1000\ W/m^2$. The diode reverse saturation current I_o is a temperature dependent quantity:

$$\frac{I_o}{I_{o,ref}} = \left(\frac{T_c}{T_{c,ref}} \right)^3 \tag{4}$$

Equation 4 gives the current implicity as a function of voltage. Once I_L and I_o are found from Equations 3 and 4, Newton's method is employed to calculate the PV current. In addition, an iterative search routine finds the current I_{mp} and voltage V_{mp} at the point of maximum power (mp) along the IV curve.

The needed parameter to complete the time step calculation process include several values which must be read from manufacturers' PV module catalogs. The manufactures' values are used to determine the equivalent circuit characteristics $I_{L,ref}$, $I_{o,ref}$, γ, and R_s. These characteristics define an equivalent circuit that is employed to find the PV performance at each time step. More information about the algebra and calculation algorithms used to solve for the four equivalent circuit characteristics can be found in (Solar Energy Laboratory, 2007).

2.2 Module Operating Temperature (Thermal Model)

The PV calculation algorithm uses temperature data from the standard $NOCT$ (Nominal Operating Cell Temperature) measurements to compute the module temperature T_c at each time step. The NOCT temperature ($T_{c,NOCT}$) is the module operating temperature at a $1m/s$ wind speed, no electrical load, and a certain specified insolation and ambient temperature (Duffie and Beckman, 1991).

The NOCT conditions also depend on the type of the considered PV module. They can be entered by the user through the software interface or, for standard technologies, are assumed the values given in (CETC, 2004).

The values for insolation $G_{T,NOCT}$ and ambient temperature $T_{a,NOCT}$ are usually $800\,W/m^2$ and $20°C$. The NOCT data will be used to determine the ratio of the module transmittance-reflectance product to the module loss coefficient:

$$\frac{\tau\alpha}{U_L} = \frac{(T_{c,NOCT} - T_{a,NOCT})}{G_{T,NOCT}} \tag{5}$$

Assuming $\tau\alpha/U_L$ ratio is constant, the module temperature at any time step is:

$$T_c = T_a + \frac{(G_T T_{c,NOCT} - T_{a,NOCT})}{G_{T,NOCT} \left(1.0 - \frac{\eta_{c,ref}}{\tau\alpha}\right)} \tag{6}$$

where:

$$\eta_{c,ref} = \frac{I_{MR}\, V_{MR}}{G_{T,ref}} \tag{7}$$

$\eta_{c,ref}$ is a reference conversion efficiency of the module which varies with ambient conditions. V_{MR} is the reference maximum power Voltage (V) and I_{MR} is the reference current at maximum power (A). The value of $\tau\alpha$ may be either a constant or calculated from an incidence angle correlation, as described in the following section.

2.3 Incidence Angle Modifier Correlation

The implemented algorithm includes an "incidence angle modifier" routine. If this routine is selected by the user, an empirical correlation determines the transmittance-reflectance product ($\tau\alpha$) of the module at each time step according to the sun position in the sky. This calculation is based on the module slope, on the angle of incidence and on the intensity of each radiation component (direct, diffuse, and ground-reflected). Considering the product $\tau\alpha$ for normal incidence angle as input parameter, using the incidence angle modifier will always produce a more conservative (and probably more accurate) estimate of system performance. For most locations, a given PV array will generate about 10% less energy over the course of an year when the incidence angle routine is enabled. $\tau\alpha$ at normal incidence is not usually included in the list of manufacturer's parameters, although 0.9 is usually a good estimate (Solar Energy Laboratory, 2007).

Whether or not the modifier is used, the radiation incident on the PV Panel is always multiplied by $\tau\alpha$ to account for reflective losses before Equation 3 is used to determine the photocurrent. The expression for the incidence angle modifier (IAM), taken from (King *et al.*, 1997) is:

$$IAM = 1 - (1.098 \times 10^{-4})\xi - (6.267 \times 10^{-6})\xi^2 + (6.583 \times 10^{-7})\xi^3 - (1.4272 \times 10^{-8})\xi^4 \tag{8}$$

where,

$$IAM = \frac{\tau\alpha}{\tau\alpha_{normal}} \tag{9}$$

Here, ξ is the angle of incidence in degrees, with $\xi = 0°$ indicating normal incidence. In Fig. 3, the incidence angle modifier (IAM) variations as function of θ have been presented.

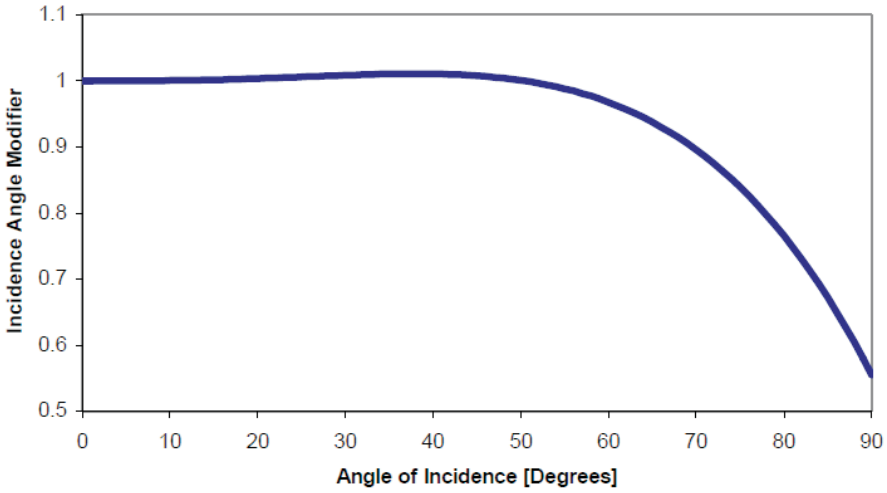

Figure 3. Incidence Angle Modifier of King *et al.*, 1997.

The angle of incidence for the beam component of the solar radiation is obtained directly the PowerDomus. However, the software does not calculate effective angles of incidence for the diffuse and ground-reflected radiation components. In this way, the photovoltaic module uses two additional correlations to find these effective angles of incidence. These correlations, developed by Duffie and Beckman (Duffie and Beckman, 1991), are:

$$\theta_{eff,diff} = 59.7 - 0.1388\omega + 0.001497\omega^2 \tag{10}$$

$$\theta_{eff,gnd} = 90 - 0.5788\omega + 0.002693\omega^2 \tag{11}$$

where ω is the slope of the PV array in degrees. In the case of PowerDomus application, this value will be equal to the surface slope. The total insolation on the array is found by summing the individual radiation components and multiplying them by their appropriate incidence angle modifiers:

$$G_{T,eff} = \tau\alpha_{norm}(G_{T,beam}IAM_{beam} + G_{T,diff}IAM_{diff} + G_{T,gnd}IAM_{gnd}) \tag{12}$$

3. BUILDING HYGROTHERMAL MODEL

In the present work, a lumped formulation for calculating both room air temperature and humidity ratio is considered for each building zone.

Equation 13 describes the energy balance, for a building room submitted to loads of conduction, convection, short-wave solar radiation, inter-surface long-wave radiation, infiltration, ventilation and the sensible and cooling loads for the HVAC system.

$$\dot{E}_t + \dot{E}_g = \rho_{air}\, c_{P\,air}\, V_{room} \frac{\mathrm{d}T_i}{\mathrm{d}t} \tag{13}$$

where $\dot{E}_t$ is the energy transfer rate that crosses the room control surface (W), $\dot{E}_g$ is the internal energy generation rate (W), ρ_{air} is the air density (kg/m^3), $c_{P,\,air}$ is the specific heat of air ($J/(kg\ K)$), V_{room} is the room volume (m^3) and $\mathrm{d}T_i$ is the room air temperature ($^\circ C$).

The term $\dot{E}_t$, on the energy conservation equation, includes loads associated to the building envelope (sensible and latent conduction heat transfer), furniture (sensible and latent), fenestration (conduction and solar radiation), openings (ventilation and infiltration) and HVAC systems. The term $\dot{E}_g$ accounts for the internal heat gain from people, equipment and lighting.

The sensible and latent loads associated to the combined heat and moisture transfer problem through the building zone porous walls are calculated as:

$$Q_{wall,S}(t) = \sum_{j=1}^{m} h_{c,j}\, A_{surf,\,j}[T_{j,x=L}(t) - T_j(t)] \tag{14}$$

$$Q_{wall,L}(t) = \sum_{j=1}^{m} L(T_{j,x=L}(t)) h_{m,j}\, A_{surf,\,j}[\rho_{v,n,j=L}(t) - \rho_{v,int}(t)] \tag{15}$$

In Equations 14 and 15, $A_{surf,\,j}$ represents the area of the j-th surface (m^2), h_c is the convective transfer coefficients for heat ($W/m^2\ K$) and h_m for mass (m/s), $T_j(t)$ the temperature at the j^{th} internal surface of the considered zone (K), L the vaporization latent heat (J/kg) and ρ_v the water vapor density (kg/m^3).

The temperature and the vapor density distributions needed to determine the sensible and latent conduction loads given by Equations 14 and 15 are calculated by using the combined heat and moisture transfer model based on the Philip and DeVries theory (Philip and De Vries, 1957) and the method presented in (Mendes *et al.*, 2002), which solves the following set of partial different governing equations for each control volume within the porous building element:

$$\rho_0\, c_{P,\,M}(T,\theta)\frac{\partial T}{\partial t} = \frac{\partial}{\partial x}\left(\lambda(T,\theta)\frac{\partial T}{\partial x}\right) + L(T)\rho_1 \frac{\partial}{\partial x}\left(D_{TV}(T,\theta)\frac{\partial T}{\partial x} + D_{\theta V}(T,\theta)\frac{\partial \theta}{\partial x}\right) \tag{16}$$

$$\frac{\partial \theta}{\partial T} = \frac{\partial}{\partial x}\left(D_T(T,\theta)\frac{\partial T}{\partial x} + D_\theta(T,\theta)\frac{\partial \theta}{\partial x}\right) \tag{17}$$

where ρ_0 is the solid matrix density, $c_{P,\,M}$ the mean specific heat, T the temperature (K), t the time (s), λ the thermal conductivity ($W/m^2\ K$), L the latent heat of vaporization ($= h_{LV}$), θ the volume basis moisture content (m^3/m^3), j_v the vapor flow ($kg/(m^2\ s)$), ρ_l the water density, D_{TV} the vapor phase transport coefficient associated to a temperature gradient ($m^2/(s\,K)$), $D_{\theta V}$ the vapor phase transport coefficient associated to a moisture content gradient (m^2/s), D_T the moisture transport coefficient associated to a temperature gradient ($m^2/s\ K$) and D_θ the moisture transport coefficient associated to a moisture content gradient (m^2/s).

Internally, the wall is exposed to convection and phase change, and externally ($x = 0$), it is exposed to solar radiation ($\alpha\, G_T$), convection ($h_{c,e}(T_e - T(0))$) and phase change ($h_{m,e}(\rho_{v,e} - \rho v, x = 0)$), so that the energy equation becomes:

$$-\left(\lambda(T,\theta)\frac{\partial T}{\partial x}\right)_{x=0} - (L(T)\ j_v)_{x=0} = h_{ext}(T_{ext} - T_{x=0}) + \alpha\ G_T + L(T)\ h_{m,ext}(\rho_{v,ext} - \rho_{v,x=0}) \tag{18}$$

The conservation governing equations are then discretized by using the control-volume formulation method with a central difference scheme and linearized vapor concentration difference at the boundaries in terms of temperature and moisture content. The resulting algebraic equations are solved using the MultiTriDiagonal Matrix Algorithm (MTDMA) as described in (Mendes and Philippi, 2004).

The building zone model has to be fed with the sensible and latent HVAC system cooling loads, while the HVAC model needs the zone leaving air psychrometric state and the airflow return rate.

In terms of water vapor balance, different contributions have been considered: ventilation, infiltration, internal generation, porous walls, furniture, HVAC system and people breath. In this way, the lumped formulation becomes:

$$(\dot{m}_{inf} + \dot{m}_{vent})(w_e - w_i) + J_b + J_{ger} + J_{porous\ surface} + J_{HVAC} = \rho_{air}\ V_{air} \frac{\mathrm{d}w_i}{\mathrm{d}t} \tag{19}$$

In the water vapor mass balance (Equation 19), the term $\dot{m}_{inf}$ is the mass flow by infiltration (kg/s), $\dot{m}_{vent}$ corresponds to the mass flow by ventilation (kg/s) and w_i and w_e are the internal and external humidity ratio (kg water/kg dry air), respectively. The term J_{HVAC} is calculated as:

$$J_{HVAC} = \dot{m}_{inf}(w_{inf} - w_{int}) \tag{20}$$

and the term $J_{porous\ surface}$ is calculated in the same way as the latent conduction load.

The room air temperature (T_i) is calculated by the energy conservation equation (Equation 13), while the supply air temperature (T_{inf}) is calculated by using the equations that compose the secondary system, in general applications it will be the models for the mixing box, cooling and dehumidification coil, humidifier and fan.

4. INTEGRATION TO THE BUILDING STRUCTURE

By using the PowerDomus software, the user can select any building zone external surface to add photovoltaic panels to the building envelope as building-integrated photovoltaic strategy. In this way, the wall layer materials will still be considered and additional calculations will be performed in order to simulate the whole-building and energy effect of photovoltaic panels by changing the boundary conditions on the external surface. The following sections describe how the PV modules affect the heat and mass transfer to an specific region on the building wall.

Based on two simulation parameters that are offered to the users, PowerDomus can simulate just the building energy calculation or the whole-building hygrothermal model, according to the user needs. Following this configuration, two options of building-integrated photovoltaic systems have also been implemented and both heat and mass transfer can be considered.

4.1 Energy Model

At the external free surfaces, the wall material is exposed to convection heat and mass transfers and phase change so that the boundary condition energy conservation equation has already been presented in Equation 18.

When photovoltaic solar panels are considered, an additional thermal resistance will be created in the external layer and the heat flux will be modified according to the photovoltaic panel efficiency (η_c). The amount of solar energy that was not converted into electrical power by the silicon cells will be conducted as a heat ($E_{conducted}$) according to Equation 21.

$$E_{conducted} = (1 - \eta_c)\tau_{glass}\ \alpha_c\ G_{T,eff} \tag{21}$$

In Equation 21, τ_{glass} is the glass transmitance and α_c is the cell absorptance. Equation 22 shows the thermal resistance caused by the PV panel, where a correction for the convective heat transfer coefficient is presented.

$$\frac{1}{\bar{h}_{c,e}} = \frac{1}{h_{c,e}} + \frac{e_{glass}}{\lambda_{glass}} \tag{22}$$

where $\bar{h}_{c,e}$ is the corrected convection heat transfer coefficient on the building external surface ($W/m^2\ K$), e_{glass} is the glass thickness (m) and λ_{glass} is the glass thermal conductivity.

4.2 Moisture Model

When the mass transfer is taken into account under the photovoltaic panel, the panel itself is considered as an impermeable boundary condition for moisture transfer. In this way, Equation 23 which represents the mass balance at the surface and Equation 18 which represents the energy balance will then be modified under the panel region, where the mass transfer convection coefficient - h_m - will be neglected.

$$-\frac{\partial}{\partial x}\left(D_\theta(T,\theta)\frac{\partial \theta}{\partial x} + D_T(T,\theta)\frac{\partial T}{\partial x}\right)_{x=0} = 0 \tag{23}$$

Important considerations about the difficulties (additional uncertainties) on the integration of the PV array and the building structure can be made:

- There is a lack of information on the contact resistance between the panel and the building envelope;
- The unidimensional characteristics of the heat and moisture model implemented into PowerDomus neglect the heat flux between the region area without PV and the area covered by the PV array.

5. VERIFICATION PROCEDURES

This section shows the verification procedures of the PV algorithm implemented into PowerDomus. Comparisons between PowerDomus and TRNSYS in terms of the amount of energy converted into electrical power by the "four-parameter" algorithm are described in the sequence. The following sections describe the simulation parameters and the results when using or not using the incidence angle modifier correlation.

5.1 Simulation Parameters

The first parameter to be selected is a typical weather file that could be used by all programs. Here, the TMY2 weather file for Denver city, USA, has been adopted (US Department of Energy, 2006). This weather condition has been considered because it has already been used as standard for building and energy simulation tests - BESTEST (Judkoff and Neymark, 1995).

After the definition of test climatic conditions, the photovoltaic panel has to be selected. Any PV panel can be used since their thermal and energy characteristics were available. Tab. 1 shows the panel characteristics adopted here. More information can be found in (BP SOLAR, 2007), where the panel technical brochure is presented.

Table 1. Photovoltaic panel electrical characteristics.

Electrical Characteristics	Values
Nominal Voltage	$12\ V$
Maximum power (P_{max})	$50\ W$
Voltage at P_{max} (V_{mp})	$17.5\ V$
Current at P_{max} (I_{mp})	$2.9\ A$
Warranted minimum P_{max}	$45\ W$
Short-circuit current (I_{sc})	$3.2\ A$
Open-circuit voltage (V_{oc})	$21.8\ V$
Temperature coefficient of I_{sc}	$(0.065 \pm 0.015)\ \%/°C$
Temperature coefficient of V_{oc}	$-(80 \pm 10)\ mV/°C$
Temperature coefficient of power	$-(0.5 \pm 0.05)\ \%/°C$
NOCT	(Air $20°C$; Sun $0.8\ kW/m^2$; wind $1\ m/s$) $47 \pm 2°C$
Maximum series fuse rating	$20\ A$
Maximum system voltage	$50\ V$

The selected panel has also $0.839\ m \times 0.537\ m$ of length and width, respectively, and weights $6.0\ kg$. It has 72 solar cells distributed in a 4×18 matrix connected in two parallel strings of 36. The construction characteristics are: a high-transmission tempered $3\text{-}mm$ glass out the front and white polyester at the rear part. The panel glass properties are presented in Tab. 2. Moreover, the value of 0.95 for the cell solar absorptance has been considered.

Table 2. Glass characteristics.

Property	Value
Thickness (e)	$0.003048\ m$
Thermal conductivity (λ)	$1.0\ W/m^2\ K$
Transmitance (τ)	0.84

In the following tests two panels in parallel configuration have been simulated maintaining $12\ V$ at the array output.

5.2 Array Conversion

After the simulation parameters description, this section reports the comparison results between PowerDomus and TRNSYS software considering the amount of solar energy that was converted to electrical power. Figure 4 shows a comparison between PowerDomus and TRNSYS for the first week of January and for the first week of July, *i.e.*, winter and summer periods.

In Fig. 4, a good agreement between PowerDomus and TRNSYS results is verified when the array output energy generation is compared. The differences between TRNSYS and PowerDomus, that have been illustrated in Fig. 4, correspond to a yearly 6.09% more energy conversion for TRNSYS when compared to the the results presented for the PowerDomus simulation tool.

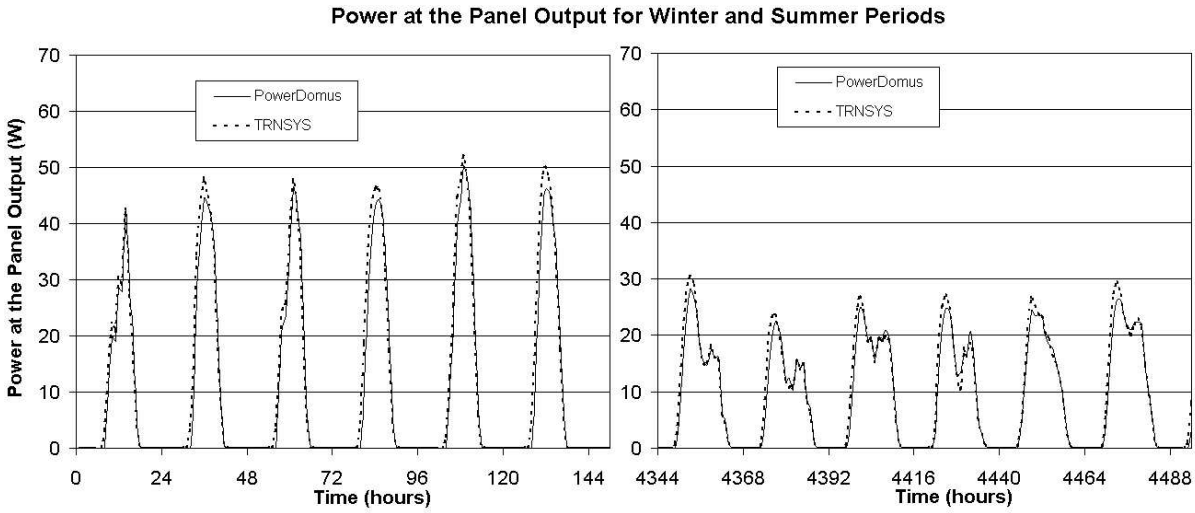

Figure 4. Energy conversion comparisons when incidence angle modifier is not considered.

5.3 Array Conversion Considering the Incidence Angle Modifier Correlation

The incidence angle modifier correlation algorithm, which has been described in Section 2.3 has been considered in this section and comparisons between PowerDomus and TRNSYS results have been performed in terms of array output energy generation.

Performing the same comparison as the one presented in Fig. 4, where the incidence angle modifier correlation has not been used, it is possible to evaluate the influences of this algorithm and its influences on the correction of the array converted energy of both software.

Figure 5 reports the comparisons between TRNSYS and PowerDomus by using the same simulation parameters presented in Section 5.1. In terms of agreement between PowerDomus and PVSYST results, it can be noticed that the use of the incidence angle modifier contributes to reduce de differences between the two software. However, it also can be verified that a slight reduction on the energy conversion has been verified and that the influences of the incidence angle modifier when Denver climate conditions have been adopted are more relevant during cold seasons.

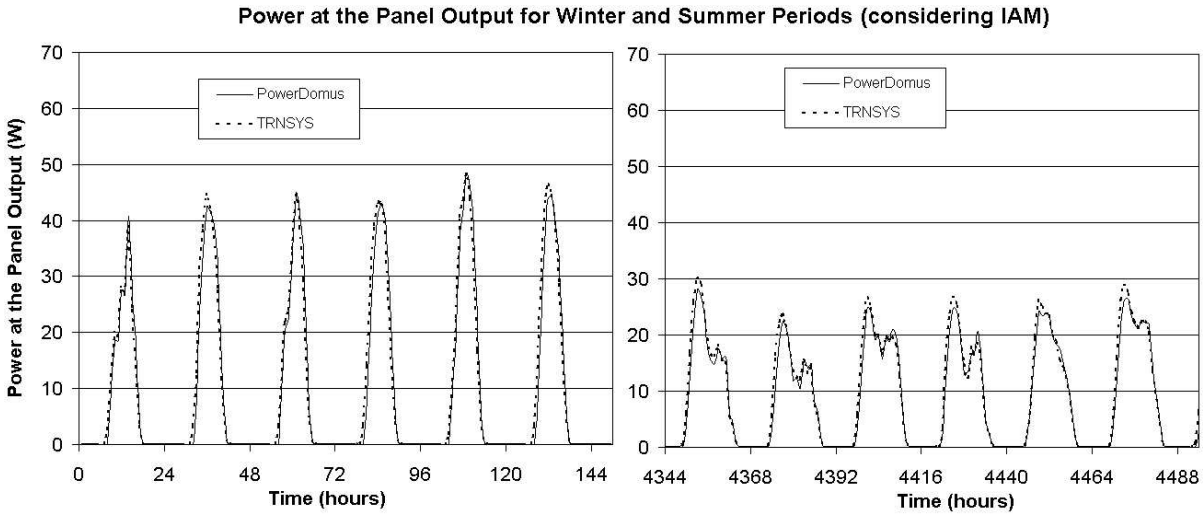

Figure 5. Energy conversion comparisons considering incidence angle modifier.

When the incidence angle modifier correlation is considered in both software, the differences between TRNSYS and PowerDomus, that have presented in Fig. 5, present significant reduction. In this case, just a yearly 3.49% more energy conversion for TRNSYS is verified.

Comparing the results presented in Fig. 4 and 5, the monthly converted power differences between TRNSYS and PowerDomus in the PV array with and without considering the incidence angle modifier correlation are presented in Tab. 3. The term IAM described in Tab. 3 means incidence angle modifier correlation. Higher differences between the amount of energy converted by the PV panels are presented in the winter period and the converted power values provided by TRNSYS are always higher than PowerDomus.

Table 3. Monthly converted power differences between TRNSYS and PowerDomus when the incidence angle modifier correlation is adopted.

	Differences(%)	
Month	without IAM	with IAM
1	6.75	2.74
2	6.04	2.21
3	5.70	2.55
4	5.91	3.32
5	5.19	3.11
6	4.97	3.62
7	4.75	4.05
8	6.04	4.85
9	6.15	3.97
10	7.92	4.81
11	7.18	3.27
12	7.78	3.77

6. CONCLUSIONS

This work described the coupling of photovoltaic panels into a whole-building and energy simulation software - PowerDomus. Considering that PowerDomus provides two simulation possibilities based on two model types: one considering just the purely conductive heat transfer, which is based on Fourier's law and neglects any moisture desorption/adsorption effect, and a the second one (a combined heat and moisture transport model), which considers the coupled heat and moisture transport through the building envelop, the integration of photovoltaic modules presented in this work followed the same structure.

Results were divided into two main sections: the first section described the photovoltaic system verification without using the incidence angle modifier correlation and, in the sequence, results showing the influences of the incidence angle modifier correlation have also been reported and compared to the results obtained by using the TRNSYS software. Good agreement have been obtained between PowerDomus and TRNSYS result considering the quantity of parameters that must be configured for photovoltaic simulation.

The main idea for future works is to show the hygrothermal effects of the photovoltaic integration and to discuss the influences of BIPV systems on the building hygrothermal behavior and in the occupants thermal comfort sensation.

7. ACKNOWLEDGEMENTS

The authors thank CAPES (*Coordenação de Aperfeiçoamento de Pessoal de Nível Superior*) of the Secretariat of Education of Brazil, FINEP (*Financiadora de Estudos e Projetos*) and CNPq (*Conselho Nacional de Desenvolvimento Científico e Tecnológico*) of the Secretariat of Science and Technology of Brazil for support of this work.

8. REFERENCES

BP SOLAR, 2007, BP 350 High-efficiency photovoltaic module using silicon nitride multicrystalline silicon cells, Technical report, BP, [http://www.bp.com], acessed in January, 2010.

CETC, 2004, "Clean Energy Project Analysis: RETScreen Engineering & Cases Textbook - Photovoltaic Project Analysis", Minister of Natural Resources Canada, Varennes, Canada.

Davis, W. M., Fanney, A. H., and Dougherty, B. P., 2002, Evaluating Building Integrated Photovoltaic Performance Models, "Proc. of the 29th IEEE Photovoltaic Specialists Conference (PVSC)", New Orleans, Louisiana, USA.

Duffie, J. A. and Beckman, W. A., 1991, "Solar Engineering of Thermal Processes", John Wiley Son, Inc., New York.

Eckstein, J. H., 1990, Detailed Modeling of Photovoltaic Components, Master's thesis, Solar Energy Laboratory, University of Wisconsin, Madison.

EPE, 2009, Brazilian Energy Balance - 2009, Technical report, Empresa de Pesquisa Energética and Ministério de Minas e Energia - MME.

Friling, N., Jiménez, M. J., Bloem, H., and Madsen, H., 2009, Modelling the Heat Dynamics of Building Integrated and Ventilated Photovoltaic Modules, "Energy and Buildings", , No. 41, pp. 1051–1057.

Griffith, B. and Ellis, P., 2004, Photovoltaic and Solar Thermal Modeling with the EnergyPlus Calculation Engine, Technical report, National Renewable Energy Laboratory, Denver, Colorado.

ISE, 2008, PVSYST 5.06 - Software for photovoltaic Systems, [http://www.pvsyst.com], acessed in March, 2008.

Judkoff, R. D. and Neymark, J. S., 1995, Colorado National Renewable Energy Laboratory, NREL/TP-472-6231.

King, D. L., Kratochvil, J. A., and Boyson, W. E., 1997, Measuring the Solar Spectral and Angle-of-Incidence Effects on Photovoltaic Modules and Irradiance Sensors, "Proceedings of the 1994 IEEE Photovoltaics Specialists Conference", pp. 1113–1116.

Mendes, N., Oliveira, R. C. L. F., and Santos, G. H., 2003, A Whole-Building Hygrothermal Simulation Program, "Proc. of the Eighth Building Simulation Conference (IBPSA'03)", Vol. 1, pp. 863–870, Eindhoven, Netherlands.

Mendes, N., Philippi, P., and Lamberts, R., 2002, A New Mathematical Method to Solve Highly-Coupled Equations of Heat and Mass Transfer in Porous Media, "International Journal of Heat and Mass Transfer", Vol. 45, No. 3, pp. 509–518.

Mendes, N. and Philippi, P. C., 2004, MultiTriDiagonal-Matrix Algorithm for Coupled Heat Transfer in Porous Media: Stability Analysis and Computational Performance, "Journal of Porous Media", Vol. 7, No. 3, pp. 193–211.

Ordenes, M., Marinoski, L., Braun, P., and Rüther, R., 2007, The Impact of Building-Integrated Photovoltaics on the Energy Demand of Multi-Family dwellings in Brazil, "Energy and Buildings", , No. 39, pp. 629–642.

PHANTASM, 1999, Photovoltaic Analysis and TrAnsient Simulation Method (PHANTASM), Building Integrated Photovoltaic Simulation Software, Technical report, Solar Energy Laboratory, University of Wisconsin, Madison, Wisconsin, USA.

Philip, J. R. and De Vries, D. A., 1957, Moisture Mouvement in Porous Material Under Temperature Gradients, "Transactions of the American Geophysical Union", Vol. 38, No. 2, pp. 222–232.

Qiu, Z., Chow, T., Li, P., Li, C., Ren, J., and Wang, W., 2009, Performance Evaluation of the Photovoltaic Double-Skin Facade, "Proc. of the 11^{th} International IBPSA Conference (BS'2009)", pp. 2251–2257, Glasgow, Scotland.

Silva, F. D. L. and Beyer, P. O., 2008, Análise de uma Simulação Computacional de um Ambiente Climatizado Alimentado pela rede Elétrica Convencional e por Painéis Solares Fotovoltaicos, "Proc. of the Congresso de Ar Condicionado, Refrigeração, Aquecimento e Ventilação do Mercosul (MERCOFRIO'08)".

Solar Energy Laboratory, 2007, TRNSYS 16: a TRaNsient SYstem Simulation program - Mathematical Reference, Technical Report Volume 5, Solar Energy Laboratory, University of Wisconsin, Madison.

Townsend, T. U., 1989, A Method for Estimating the Long-Term Performance of Direct-Coupled Photovoltaic Systems, Master's thesis, Solar Energy Laboratory, University of Wisconsin, Madison.

US Department of Energy, 2006, Information Resources - EnergyPlus Energy Simulation Software, Technical report, Building Technologies Program from the US Department of Energy, [http://apps1.eere.energy.gov/buildings/energyplus/], acessed in December, 2006.

9. Responsibility notice

The authors are the only responsible for the printed material included in this paper.